Lung Cancer 130 (2019) 169–178

Contents lists available at ScienceDirect

Lung Cancer

journal homepage: www.elsevier.com/locate/lungcan

IKKβ targeting reduces KRAS-induced lung cancer angiogenesis *in vitro* and *in vivo*: A potential anti-angiogenic therapeutic target

Tatiana Correa Carneiro-Lobo[a], Luiza Coimbra Scalabrini[a], Leila da Silva Magalhães[a], Laura B. Cardeal[a], Felipe Silva Rodrigues[a], Edmilson Ozorio dos Santos[a], Albert S. Baldwin[b], Elena Levantini[c,d], Ricardo J. Giordano[a], Daniela Sanchez Bassères[a,*]

[a] Chemistry Institute, Department of Biochemistry, University of São Paulo, São Paulo, Brazil
[b] Lineberger Comprehensive Cancer Center, University of North Carolina at Chapel Hill, Chapel Hill, NC, USA
[c] Beth Israel Deaconess Medical Center, Harvard Medical School, Boston, MA, USA
[d] Institute of Biomedical Technologies, National Research Council (CNR), Pisa, Italy

ARTICLE INFO

Keywords:
Angiogenesis
KRAS
IKKβ
Lung cancer
IL-8
VEGF
Therapeutic target

ABSTRACT

Objectives: The ability of tumor cells to drive angiogenesis is an important cancer hallmark that positively correlates with metastatic potential and poor prognosis. Therefore, targeting angiogenesis is a rational therapeutic approach and dissecting proangiogenic pathways is important, particularly for malignancies driven by oncogenic KRAS, which are widespread and lack effective targeted therapies. Based on published studies showing that oncogenic RAS promotes angiogenesis by upregulating the proangiogenic NF-κB target genes IL-8 and VEGF, that NF-κB activation by KRAS requires the IKKβ kinase, and that targeting IKKβ reduces KRAS-induced lung tumor growth *in vivo*, but has limited effects on cell growth *in vitro*, we hypothesized that IKKβ targeting would reduce lung tumor growth by inhibiting KRAS-induced angiogenesis.

Materials and methods: To test this hypothesis, we targeted IKKβ in KRAS-mutant lung cancer cell lines either by siRNA-mediated transfection or by treatment with Compound A (CmpdA), a highly specific IKKβ inhibitor, and used *in vitro* and *in vivo* assays to evaluate angiogenesis.

Results and conclusions: Both pharmacological and siRNA-mediated IKKβ targeting in lung cells reduced expression and secretion of NF-κB-regulated proangiogenic factors IL-8 and VEGF. Moreover, conditioned media from IKKβ-targeted lung cells reduced human umbilical vein endothelial cell (HUVEC) migration, invasion and tube formation *in vitro*. Furthermore, siRNA-mediated IKKβ inhibition reduced xenograft tumor growth and vascularity *in vivo*. Finally, IKKβ inhibition also affects endothelial cell function in a cancer-independent manner, as IKKβ inhibition reduced pathological retinal angiogenesis in a mouse model of oxygen-induced retinopathy. Taken together, these results provide a novel mechanistic understanding of how the IKKβ pathway affects human lung tumorigenesis, indicating that IKKβ promotes KRAS-induced angiogenesis both by cancer cell-intrinsic and cancer cell-independent mechanisms, which strongly suggests IKKβ inhibition as a promising antiangiogenic approach to be explored for KRAS-induced lung cancer therapy.

1. Introduction

Lung cancer is the leading cause of cancer-related deaths worldwide and KRAS-mutant lung cancers account for approximately 25% of non-small cell lung carcinomas [1,2]. As with other KRAS-driven malignancies, KRAS-driven lung cancer lacks specific targeted therapies [3,4]. Most strategies currently being pursued to target KRAS involve inhibiting effectors that promote proliferation and survival, proteins that display synthetic lethality with mutant KRAS and proteins involved in mediating KRAS-induced metabolic changes [5–7]. Interestingly, KRAS-targets involved in promoting tumor angiogenesis remain underexplored. This is surprising given the fact that the ability to drive angiogenesis is crucial, not only for primary tumor growth, but also for metastatic dissemination. Therefore, characterization of novel druggable targets involved in promoting KRAS-induced angiogenesis could lead to novel therapeutic alternatives for lung cancer, as well as other

* Corresponding author at: Department of Biochemistry, Chemistry Institute, University of São Paulo, Av. Prof. Lineu Prestes 748, Bloco 12 inferior, sala 1200, 05508-000, São Paulo, SP, Brazil.
E-mail address: basseres@iq.usp.br (D.S. Bassères).

https://doi.org/10.1016/j.lungcan.2019.02.027
Received 15 October 2018; Received in revised form 14 February 2019; Accepted 25 February 2019

RAS-driven cancers.

Oncogenic Ras not only initiates tumor formation by stimulating proliferation, but also ensures tumor progression by promoting tumor angiogenesis [8,9]. Different pathways downstream of oncogenic Ras have been implicated in promoting tumor angiogenesis ultimately by leading to transcriptional upregulation of vascular endothelial growth factor (VEGF) and CXC chemokine interleukin-8 (IL-8) [8,10–13]. Both VEGF and IL-8 have been shown to play an essential role in tumor angiogenesis mediated by Ras [10,14,15]. VEGF inhibition by antisense technology in KRAS-mutated colon cancer cell lines blocks their ability to form xenograft tumors, whereas VEGF expression in nontumorigenic KRAS wildtype isogenic cell lines partially restores their tumorigenicity [14]. In addition, when compared to HRAS-transformed wildtype murine embryonic fibroblasts (MEFs), HRAS-transformed VEGF null MEFS display impaired ability to grow as fibrosarcomas *in vivo* due to reduced vascular density and permeability [15]. Finally, inhibition of oncogenic Ras expression or administration of an IL-8 neutralizing antibody in $HRAS^{V12}$ Hela cell xenografts inhibits tumor vascularization and attenuates tumor growth [10]. Interestingly, both VEGF and IL-8 are targets of the transcription factor NF-κB [16], which, in turn, is activated by oncogenic KRAS in lung tumors *in situ* and is required for KRAS-induced lung tumorigenesis [17,18].

Canonical NF-κB activation under most circumstances is mediated by activation of the IkappaB kinase (IKK) complex, which is comprised of two catalytic subunits (IKKα and IKKβ) and a regulatory subunit (IKKγ). Once activated, the IKK complex phosphorylates the inhibitory protein IκBα (IκBα), which interacts with NF-κB and sequesters it in the cytoplasm. Upon phosphorylation by IKK, IκBα undergoes rapid ubiquitination and proteasome-mediated degradation, thereby releasing NF-κB to translocate to the nucleus where it regulates target gene transcription [16]. Not surprisingly, NF-κB activation by oncogenic KRAS in the lung involves the IKK complex. In fact, Duran et al. [19] showed that oncogenic KRAS activates the IKK complex through the signaling adaptor p62 and TRAF6. In addition, NF-κB activity in both murine and human KRAS-transformed lung cancer cells requires IKKβ kinase activity [18].

Based on this evidence, we hypothesized that targeting the IKKβ kinase, which is a druggable target in the KRAS-mediated NF-κB activation pathway, would limit lung tumor growth by inhibiting KRAS-induced angiogenesis. In support of this hypothesis, endothelial deletion of IKKβ during development leads to partial embryonic lethality due to impaired liver angiogenesis and formation of hypovascular placentae [20,21]. Adult mice with endothelial deletion of IKKβ display increased vascular permeability and decreased vascular migration capacity [21]. Finally, we and others have shown that IKKβ targeting only minimally affects KRAS-mutant lung cell growth *in vitro*, nonetheless it significantly reduces KRAS-induced lung tumor growth *in situ* [22,23].

Here, we show that VEGF and IL-8 secretion by KRAS-positive lung cancer cells requires IKKβ. Moreover, conditioned media from IKKβ-targeted KRAS-mutant lung cells reduces endothelial cell migration, invasion and tube formation *in vitro*. Furthermore, siRNA-mediated IKKβ inhibition reduces KRAS-positive lung cancer xenograft tumor growth and vascular density *in vivo*. Finally, we determined that IKKβ inhibition can affect endothelial cell function in a cancer-independent manner as well, as systemic IKKβ inhibition therapy reduces pathological retinal angiogenesis in a mouse model of neonatal retinopathy. Taken together, these results suggest that IKKβ is an important mediator of KRAS-induced angiogenesis, and that IKKβ promotes angiogenesis both by cancer cell-dependent and -independent mechanisms. Therefore, IKKβ inhibition therapy may provide a clinical therapeutic benefit for lung cancer patients harboring KRAS mutations.

2. Material and methods

2.1. Cell culture

Cell passages were kept to a minimum and no cells were passaged continuously for more than six months. Human non-small cell lung cancer cell lines harboring KRAS mutations A549 ($KRAS^{G12S}$; ATCC CCL-185) and H358 ($KRAS^{G12C}$; ATCC CRL-5807) were grown in RPMI 1640 (Thermo Fisher Scientific), supplemented with 10% (vol/vol) fetal bovine serum (FBS) (Sigma-Aldrich). Cells were treated with the highly specific IKKβ inhibitor Compound A (CmpdA) [24] (Bayer) or vehicle control dimethyl sulfoxide (0.1% DMSO) as indicated (see figure legends). HUVEC Cells (Lonza Group) were cultured at 37 °C, 5% (v/v) CO_2 in endothelial growth medium (EGM, Lonza Group) supplemented with epidermal growth factor (hEGF), vascular endothelial growth factor (VEGF), R3-insulin-like growth factor-1 (R3-IGF-1), ascorbic acid, hydrocortisone, human fibroblast growth factor β (hFGF-β), heparin, FBS, and gentamicin/amphotericin-B (GA).

2.2. siRNA transfections

Cells were seeded in 6-well-plates at a density of 1×10^5 cells/well 12 h before transfection and siRNA transfections were performed with 50 ηM of either a non-targeting siRNA control or siRNA smartpools targeting IKKβ or KRAS (Dharmacon) according to the manufacturer's instructions. Cells were collected for RNA analysis 72 h after transfection and for protein analysis 96 h after transfection.

2.3. RNA isolation and cDNA synthesis

Total RNA was isolated using Trizol reagent (Thermo Fisher Scientific) following the manufacturer's protocol. To synthesize cDNA, 1 μg RNA and Superscript III reverse transcriptase (Thermo Fisher Scientific) were used, followed by real-time PCR analysis performed in a 7300 Real-Time PCR System Step (Applied Biosystems) using SYBR® Green Master Mix (Thermo Fisher Scientific) and 200 ηM gene-specific forward or reverse primers designed using Primer Express 3 software (Applied Biosystems). The sequences used for each primer pair were as follows: IKKβ (F, 5'-GCCCTTCCTCCCCAACTG-3' and R, 5'-TCTTCTGC CGCATTTTGAA-3'), KRAS (F, 5'-CCCAGGTGCGGGAGAGA-3' and R, 5'-CAGCTCCAACTACCACAAGTTT-3'), GAPDH (F, 5'-ACCCACTCCTCCAC CTTTGA-3' and R, 5'-ACCGAGCCATTTCATTTCTG-3'), IL-8 (F, 5'-CTG GACCCCAAGGAAAACTG-3' and R, 5'-TGTGCCATCAACCTTACCAA TAA-3'); and VEGF (F, 5'-AGTGGTGAAGTTCATGGATGT-3' and R, 5'-GCACACAGGATGGTTGAAGA-3)'. Relative quantitation was performed by the ΔΔCt method using GAPDH as endogenous control.

2.4. Western blotting

Whole cell lysates were prepared using RIPA buffer (20 mM Tris–HCl pH 7.5, 150 mM NaCl, 1 mM Na_2EDTA, 1 mM EGTA, 1% NP-40) containing protease and phosphatase inhibitors (1 μg/mL leupeptin, 1% sodium deoxycholate, 2.5 mM sodium pyrophosphate, 1 mM β-glycerophosphate, 1 mM Na_3VO_4). Lysates (25 μg protein/lane) were electrophoresed in 12–15% polyacrylamide minigels, using Mini-PROTEAN® vertical electrophoresis cell (Bio-Rad). Electrophoresis was conducted with running buffer containing 25 mM Tris, 190 mM glycine, and 0.1% SDS, at 120 V for 60–90 min. Proteins were transferred to nitrocellulose membranes (Bio-Rad), with Towbin buffer (25 mM Tris, 192 mM glycine, 20% methanol) at 30 V for 16 h. Membranes were blocked with 5% BSA in TBST (20 mM Tris, pH 7.5, 150 mM NaCl, 0.1% Tween-20) for 1 h. Finally, membranes were incubated with primary antibodies, followed by incubation with fluorescently labelled secondary antibodies. Fluorescence detection was performed using ODYSSEY (Li-Cor Biosciences). The following primary antibodies were used: anti-GAPDH (Santa Cruz Biotechnology), anti-β-actin (Sigma-

Aldrich), anti-PanRAS (Merck Millipore), anti-IKKβ (Cell Signaling Technology), anti-phospho-IκBα^{Ser32} (Cell Signaling Technology) and anti-IκBα (Cell Signaling Technology). Primary antibodies were used at a dilution of 1:1000 in TBST, containing 5% BSA and 0.1% NaN_3, and incubated for 16 h at 4 °C, with the exception of the anti-β-actin antibody, that was used at a 1:7000 dilution. The following secondary antibodies were used: anti-rabbit Alexa Fluor® 680 (Thermo Fisher Scientific) and anti-mouse Alexa Fluor® 680 (Thermo Fisher Scientific). All secondary antibodies were used at a dilution of 1:15,000 in TBST and incubated for 1 h at room temperature. Protein bands of interest were quantitated by densitometry using ImageJ software, expressed relative to the endogenous control (β-actin or GAPDH) and normalized to the reference sample as indicated in the figure legends.

2.5. ELISA assay

A549 or H358 cells were transfected with siRNAs as previously described and at 96 h post-transfection, the culture medium was replaced with serum-free medium for 24 h and the culture medium was collected and stored at −80 °C until analysis. IL-8 and VEGF protein levels in the culture medium were measured by ELISA assay using commercially available CytoSet Human IL-8/CXCL8 Quantikine kit and CytoSet Human VEGF Quantikine kit (R&D Systems), respectively, as described by the manufacturer.

2.6. Migration and invasion assays

Migration assays were performed using 24-well transwell inserts with 8 μm pore membrane filters (Corning) and invasion assays were performed using matrigel-coated 24-well transwell inserts with 8 μm pore membrane filters (Corning). For both assays, conditioned medium from A549 cells transfected with a non-targeting control siRNA (siCtrl) or with siRNA smartpools targeting KRAS (siKRAS) or IKKβ (siIKKβ) was collected at 96 h post-transfection and 500 μL were added to the lower chamber to be used as chemoattractant. Supplementation of conditioned media with 5 ng/mL IL-8 and 5 ng/mL VEGF was performed as indicated. 1×10^5 HUVEC cells were resuspended in 500 μL serum-free medium, added to the upper chamber and incubated for 24 h at 37 °C in 5% CO_2. Nonmigrating cells were scraped off the upper surface of the membrane with a cotton swab, and migrating cells on the bottom surface were stained with crystal violet. Images were obtained under an IX51 Inverted Microscope (Olympus). Cells from five random fields of view from three independent experiments were counted.

2.7. Tube formation assay

Formation of capillary-like structures (tubes) was assessed in a matrigel-coated 24-well plate. Briefly, 250 μL/well of reduced growth factor matrigel (BD Biosciences) were transferred to a 24-well plate on ice and allowed to gellify at 37 °C for 30 min. A549 cells were transfected as described above with a non-targeting control siRNA (siCtrl) or with a siRNA smartpool targeting IKKβ (siIKKβ) and conditioned medium was collected at 96 h post-transfection. HUVECs were resuspended in conditioned medium as indicated above and were seeded at a density of 1×10^5 cells per well in a final volume of 300 μL and incubated at 37 °C for 6 h. Capillary-like tube formation was observed, and images were obtained under an IX51 Inverted Microscope (Olympus). Numbers of closed capillary tubes were counted in five visual fields per condition from three independent experiments.

2.8. Tumor growth assay

All animal studies were carried out in accordance with the guidelines and regulations for research and teaching involving animals of the National Counsil for Control of Animal Experimentation (Conselho Nacional de Controle de Experimentação Animal – CONCEA). The study protocols were approved by the Animal Use Ethics Committee (Comissão de Ética no Uso de Animais – CEUA) of the Chemistry Institute of the University of São Paulo. Briefly, siRNA-transfected A549 cells (1×10^6) were resuspended in 100 μL RPMI medium and subcutaneously inoculated into each flank of 6-week-old, male Balb/C nude mice in pathogen-free conditions at the University of São Paulo Chemistry Institute Animal Facility. Mice were monitored every 3 days for the appearance of tumors, and tumor volumes were determined by direct diameter measurement with a caliper. Animals were sacrificed by CO_2 euthanasia 55 days after inoculation, and tumor weight was determined. Tumor volumes were calculated using the following equation: $width^2 \times length \times 0.5$.

2.9. Immunofluorescence

Xenograft tumors were dissected, incubated for 1 h with 4% paraformaldehyde and allowed to soak in 30% sucrose overnight. Tumors were then embedded in OCT compound (Tissue-Tek) and processed into 14 μm sections using a cryostat (Microm HM 500 OMV Cryostat Microtome). Sections were air-dried for 2 h at room temperature and stored at −80 °C. On the day of the experiment, sections were rehydrated in 0.1 M phosphate buffer saline (PBS, pH 7.4) for 10 min and blocked in PBS containing 0.2% bovine serum albumin (Sigma-Aldrich) and 0.3% Triton X-100 (Sigma-Aldrich) for 1 h at room temperature. Next, for CD31 staining, sections were incubated overnight at 4 °C with 1:10 dilution of the CD31 antibody (PECAM, rat monoclonal, clone MEC13.3, BD Pharmingen), washed with PBS and incubated for 2 h at room temperature with 1:200 dilution of anti-mouse Alexa-647-conjugated secondary antibody (Jackson ImmunoResearch). Alternatively, for IKKβ staining, sections were incubated overnight at 4 °C with 1:100 dilution of the IKKβ antibody (Cell Signaling Technology), washed with PBS and incubated for 2 h at room temperature with 1:200 dilution of anti-mouse Alexa-488-conjugated secondary antibody (Jackson ImmunoResearch). Finally, slides were mounted in gel/mount (Biomeda Corp) and analyzed under an Axioskop microscope equipped with Axiocam MRc5 camera (Zeiss).

2.10. Oxygen-induced retinopathy (OIR) model analysis

A well-established mouse model of oxygen-induced retinopathy was performed as reported [25,26]. Briefly, litters of newborn C57BL/6 mice on postnatal day 7 and their mothers were placed in an airtight incubator and exposed to an atmosphere of 75% O_2 (hyperoxia) for 5 days. Incubator temperature was maintained at 23 °C, and O_2 was measured three times per day with an oxygen analyzer. On postnatal day 12, mice were returned to room air. CmpdA (10 mg/kg body weight) was administered subcutaneously or intraperitoneally on postnatal days 12, 14 and 16. Vehicle alone (DMSO) or PBS were administered similarly as controls. Animals were sacrificed by CO_2 euthanasia on postnatal day 17, the eyes were removed with a curved forceps and were immediately fixed in 4% paraformaldehyde for 30 min. Using a dissecting forceps, the cornea was cut and the retinas isolated. Retinas were then permeabilized for 30 min by incubation in PBS containing 0.5% Triton X-100 and stained with GS-IB4 isolectin conjugated to Alexa Fluor 594 (Thermo Fisher Scientific) overnight at 4 °C (10 μg/mL in PBS 0.5% Triton X-100). Under a dissecting microscope four incisions were made on the retina at 90-degree angles, forming four similarly sized quadrants united by the retina centre, the optic nerve region. The retinas were mounted on glass slides with Vectashield mounting medium (Vector Laboratories) and covered with cover slips. Images were obtained on a fluorescence zoom microscope Axio Zoom V16 (Zeiss). Quantitation of angiogenic vessels was made in Adobe Photoshop as described [25,26]. Briefly, using the polygonal lasso tool, the entire retina was selected and the total number of pixels was obtained in the histogram. Next, using the magic wand tool, the vascular area was selected, and the number of pixels was obtained. The

angiogenic area was calculated as a percentage of the total retinal area as follows: number of pixels of angiogenic vessels/number of pixels of the entire retina × 100.

2.11. Statistical analysis

All values are presented either as average ± SD or as representative images of at least three independent experiments. Statistical analysis was performed using Prism 5 (GraphPad Software). All data have been evaluated for normality of distribution. In order to assess differences within groups, we used one-way analysis of variance (ANOVA) followed by Bonferroni's multiple comparison test. For pairwise comparisons, we used a non-parametric Student's *t*-test Differences were considered statistically significant at $p < 0.05$.

3. Results

3.1. IKKβ targeting in KRAS-positive lung cells reduces IL-8 and VEGF expression and secretion

Given our hypothesis that IKKβ promotes KRAS-induced angiogenesis, which relies on KRAS-induced VEGF and IL-8 secretion [10,14], and given that VEGF and IL-8 are transcriptional targets of NF-κB [16], a transcription factor activated by oncogenic KRAS in the lung in an IKKβ-dependent manner [18], we decided to investigate whether IKKβ targeting would affect VEGF and IL-8 expression. First, we tested whether the IKKβ inhibitor CmpdA could inhibit IKKβ-mediated signaling in KRAS-mutant A549 and H358 cells. CmpdA treatment reduced phosphorylation of the IKKβ substrate IκBα while, at the same time, it increased total IκBα levels (Fig. 1a), thus confirming CmpdA's inhibitory activity. In agreement with our hypothesis, IKKβ targeting with CmpdA in A549 and H358 cells significantly reduced VEGF and IL-8 expression (Fig. 1b). Moreover, siRNA-mediated inhibition of KRAS or IKKβ expression resulted in decreased RAS protein levels and led to undetectable levels of IKKβ protein (Fig. 1c). Because the antibody used to detect RAS recognizes all three RAS isoforms (H-, K- and NRAS), we also used qPCR to evaluate the efficacy of our siRNA-mediated targeting. As can be seen in Fig. 1d, siRNA-mediated KRAS targeting in A549 and H358 cells decreased KRAS mRNA levels by 96.5% and 88.7%, respectively. siRNA-mediated IKKβ targeting in A549 and H358 cells led to a similar reduction of IKKβ mRNA levels (of 84.7% and 60.87%, respectively) (Fig. 1d). These results indicate that our siRNA-mediated silencing approach was effective. As expected, KRAS silencing reduced IL-8 mRNA expression by 70.88% and 55.01% and VEGF mRNA expression by 30.95% and 20.78% in A549 and H358 cells respectively (Fig. 1e). Consistent with the idea that IKKβ mediates KRAS-induced IL-8 and VEGF expression, siRNA-mediated IKKβ silencing in A549 and H358 cells caused a reduction in IL-8 and VEGF expression that matched the one observed by KRAS silencing: a reduction of 69.29% and 61.35% in IL-8 mRNA levels and of 21.53% and 33.18% in VEGF mRNA levels in A549 and H358 cells respectively (Fig. 1f). More meaningfully, both KRAS and IKKβ siRNA-mediated silencing in KRAS-mutant cells led to reduced VEGF and IL-8 secretion (Fig. 1g). These results indicate that IKKβ promotes KRAS-induced expression and secretion of proangiogenic factors VEGF and IL-8.

3.2. IKKβ targeting in KRAS-mutant lung cancer cells decreases endothelial cell migration, invasion and tube formation in vitro

For neovascularization to occur during tumor angiogenesis, endothelial cells have to migrate in response to proangiogenic factors and have to self-organize into tubular structures that will give rise to new vessels [27]. Since IKKβ targeting in KRAS-positive cells reduces VEGF and IL-8 secretion, we decided to investigate how IKKβ targeting in KRAS-mutant cancer cells would affect endothelial cell migration, invasion and tube formation *in vitro*. For that purpose, we evaluated human umbilical vein endothelial cells (HUVEC) migration and invasion using transwell assays, where conditioned medium from A549 cells with siRNA-mediated inhibition of KRAS or IKKβ was used as chemoattractant. Compared to conditioned medium from A549 cells transfected with a non-targeting siRNA control (siCtrl), conditioned medium from KRAS- or IKKβ-targeted A549 cells reduced HUVEC migration (Fig. 2a, upper panel) and invasion (Fig. 2b). Even though KRAS targeting was more effective than IKKβ targeting in reducing HUVEC migration (96.5% *versus* 68.19%, Fig. 2a), IKKβ targeting was more effective than KRAS targeting in reducing HUVEC invasion (60.1% *versus* 32.4%, Fig. 2b). Interestingly, supplementation of conditioned medium from KRAS- or IKKβ-targeted A549 cells with IL-8 and VEGF rescued HUVEC migration (Fig. 2a, lower panel) and similar results were obtained with H358 cells (Supplementary Fig. 1), confirming that these proangiogenic factors are involved in promoting KRAS- and IKKβ-induced endothelial cell migration and supporting a role for this pathway in promoting angiogenesis. In accordance, when compared to conditioned medium from siCtrl-transfected A549 or H358 cells, conditioned medium from IKKβ-targeted A549 or H358 cells decreased by 66.6% and 57,7%, respectively, the ability of HUVEC cells to form tubular structures *in vitro* (Fig. 2c). Even though other IKKβ-independent pathways may contribute to KRAS-induced angiogenesis, our data indicate that IKKβ is an important mediator of KRAS-induced proangiogenic effects.

3.3. siRNA-mediated IKKβ targeting in KRAS-mutant lung cancer cells reduces tumor growth and angiogenesis in vivo

We have recently shown, using a mouse model of KRAS-induced lung cancer, that IKKβ targeting with CmpdA reduces lung tumor growth and vascular density *in situ* [23]. However, as IKKβ was systemically targeted, the contribution of cancer cell-intrinsic IKKβ activity for tumor angiogenesis was not clear. More importantly, because mice do not have an IL-8 homolog [28], the contribution of this human-specific proangiogenic pathway, which is required for RAS-induced angiogenesis [10], cannot be addressed in this model. Therefore, to evaluate whether cancer cell-intrinsic IKKβ activity is required for KRAS-induced angiogenesis in human tumors, we performed xenograft studies with human A549 cells with siRNA-mediated IKKβ silencing. Even though IKKβ-targeted A549 cells still formed xenograft tumors in nude mice, when compared siCtrl-transfected A549 cells, IKKβ-targeted A549 cells formed smaller tumors (Fig. 3a). IKKβ targeting resulted in decreased tumor growth over time (Fig. 3b) and in reduced tumor weight at the endpoint (Fig. 3c). Consistent with the observed decrease in tumor growth, histologic examination of tumor tissue showed that, compared to control tumors, IKKβ-targeted tumors still displayed significantly decreased IKKβ expression (Fig. 3d). In addition, as assessed by immunofluorescence for CD31, a specific endothelial marker, IKKβ targeting reduced tumor vascular density by 52.8% (Fig. 3e). These results indicate that cancer cell-intrinsic IKKβ activity contributes to KRAS-mutant human lung tumor growth and that this reduction is associated with decreased angiogenesis.

3.4. IKKβ also affects endothelial function by cancer cell-independent pathways

In order to determine whether IKKβ can affect pathological cancer cell-independent angiogenesis *in vivo*, we used a well-established model of oxygen-induced retinopathy (OIR) caused by pathological retinal neovascularization [29,30]. This model has been widely used to study the molecular mechanisms of blood vessel formation during relative hypoxia and to assess the effect of compounds on angiogenesis [25,30,31]. To induce OIR, newborn mice are exposed to 75% oxygen from postnatal day 7 to postnatal day 12. Hyperoxia exposure causes vase-obliteration of immature retinal vessels and suppresses postnatal retinal angiogenesis, which is a natural process of murine vascular

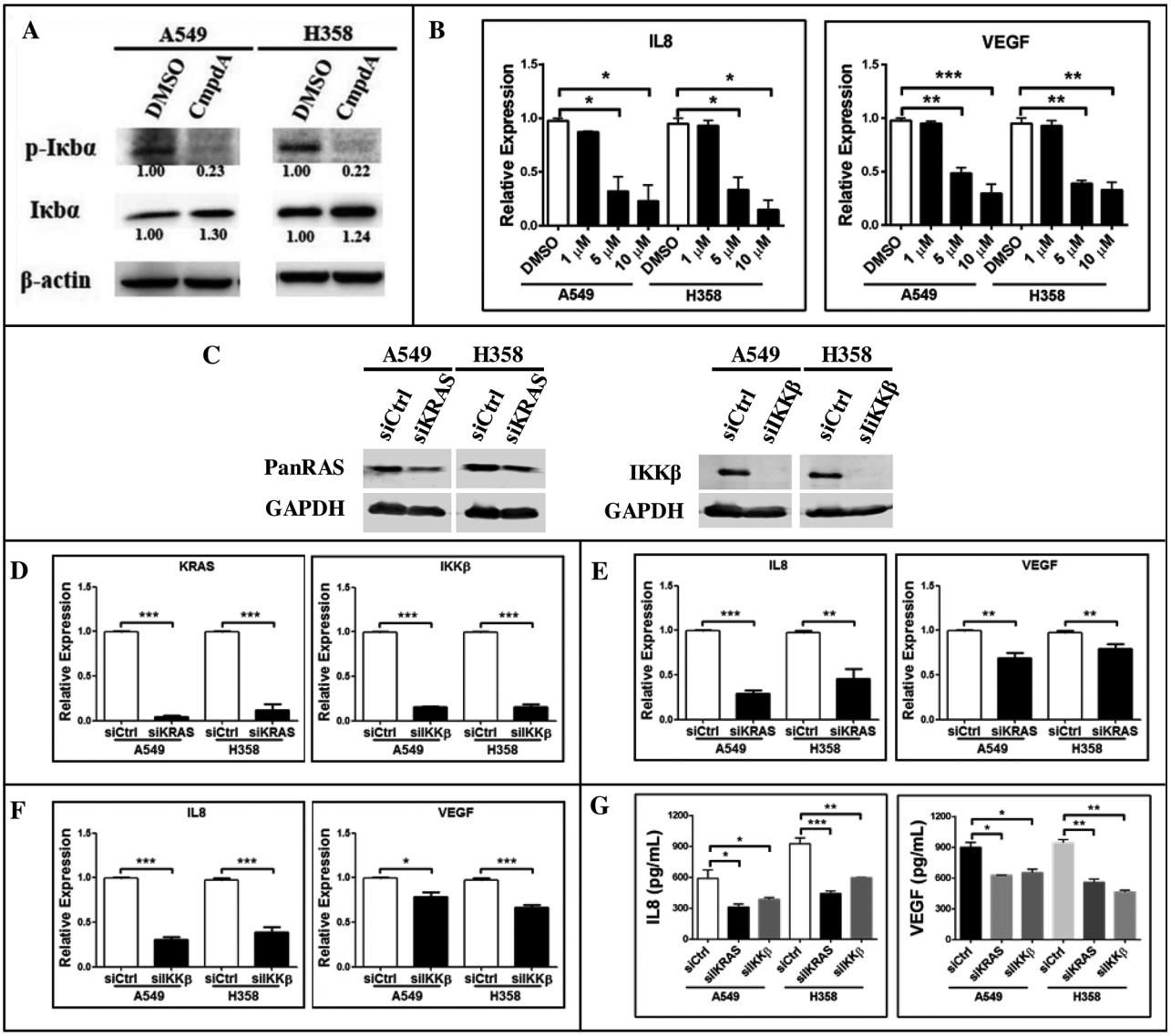

Fig. 1. IKKβ inhibition reduces IL-8 and VEGF expression and secretion. (**a**) Western Blotting of A549 and H358 cells treated with 0.1% DMSO or 5 uM CmpdA for 30 min. Antibodies used are indicated. Representative western blots are shown. Protein bands were quantitated and normalized to the reference samples (0.1% DMSO-treated samples). (**b**) A549 and H358 cells were treated with 0.1% DMSO or the indicated concentrations of CmpdA for 24 h and IL-8 and VEGF gene expression was evaluated by real-time quantitative PCR (qRT-PCR). (**c–g**) A549 and H358 cells were transfected with a non-targeting control siRNA (siCtrl) or with siRNA smartpools targeting KRAS (siKRAS) or IKKβ (siIKKβ). (**c**) Protein lysates were collected 96 h post-transfection and evaluated by Western Blotting with the indicated antibodies. (**d**) Expression of KRAS (left panel) or IKKβ (right panel) was analyzed 72 h post-transfection by qRT-PCR. (**e, f**) Expression of IL-8 (left panel) or VEGF (right panel) was analyzed 72 h post-transfection by qRT-PCR in cells transfected with siKRAS (**e**) or siIKKβ (**f**). (**g**) Conditioned culture media were collected 120 h post-transfection and protein concentrations of IL-8 and VEGF were determined by ELISA. In all cases, bar graphs represent average ± 1 s.d of three independent experiments. Statistical significance was measured by one-way ANOVA followed by Bonferroni's post-test (**b**, **g**) or by the Student's *t*-test (**d–f**) (*p < 0.05, **p < 0.01, ***p < 0.001) by comparing DMSO-treated groups with CmpdA-treated groups (**b**) or siCtrl-transfected groups with siKRAS- and/or siIKKβ-transfected groups (**d–g**). Groups being compared are indicated by horizontal bars.

retinal maturation [32]. Subsequently, mice are transferred back to normoxia. The relative reduction in oxygen levels leads to pathological retinal neovascularization, which is maximal at postnatal day 17, and regresses thereafter [25]. To evaluate whether IKKβ targeting could reduce the pathological retinal neovascularization observed in this model, mice submitted to OIR were treated with CmpdA (10 mg/kg) subcutaneously or intraperitoneally at postnatal days 12, 14 and 16. When compared with animals treated with DMSO or PBS, animals treated with CmpdA subcutaneously or intraperitoneally displayed retinas with markedly decreased vascular area (Fig. 4). These results indicate that IKKβ targeting decreases pathological retinal neovascularization *in vivo*, which suggests that IKKβ also likely contributes to angiogenesis through cancer cell-independent pathways.

4. Discussion

One of the hallmarks of cancer is the ability of cancer cells to drive tumor angiogenesis [33], which not only sustains neoplastic growth of primary tumors, but is also a feature of invasive tumors, as it is required for metastatic tumor growth [34,35]. In fact, in a wide variety of malignancies, tumor vascular density positively correlates with increased metastatic potential and poor prognosis [35]. Therefore, targeting angiogenesis is a rational approach to prevent both primary tumor growth and malignant progression, thus improving survival.

Nonetheless, safe and effective antiangiogenic strategies to treat cancer patients have not yet been translated into the clinic [34]. For example, tumor response to therapies targeting the VEGF signaling

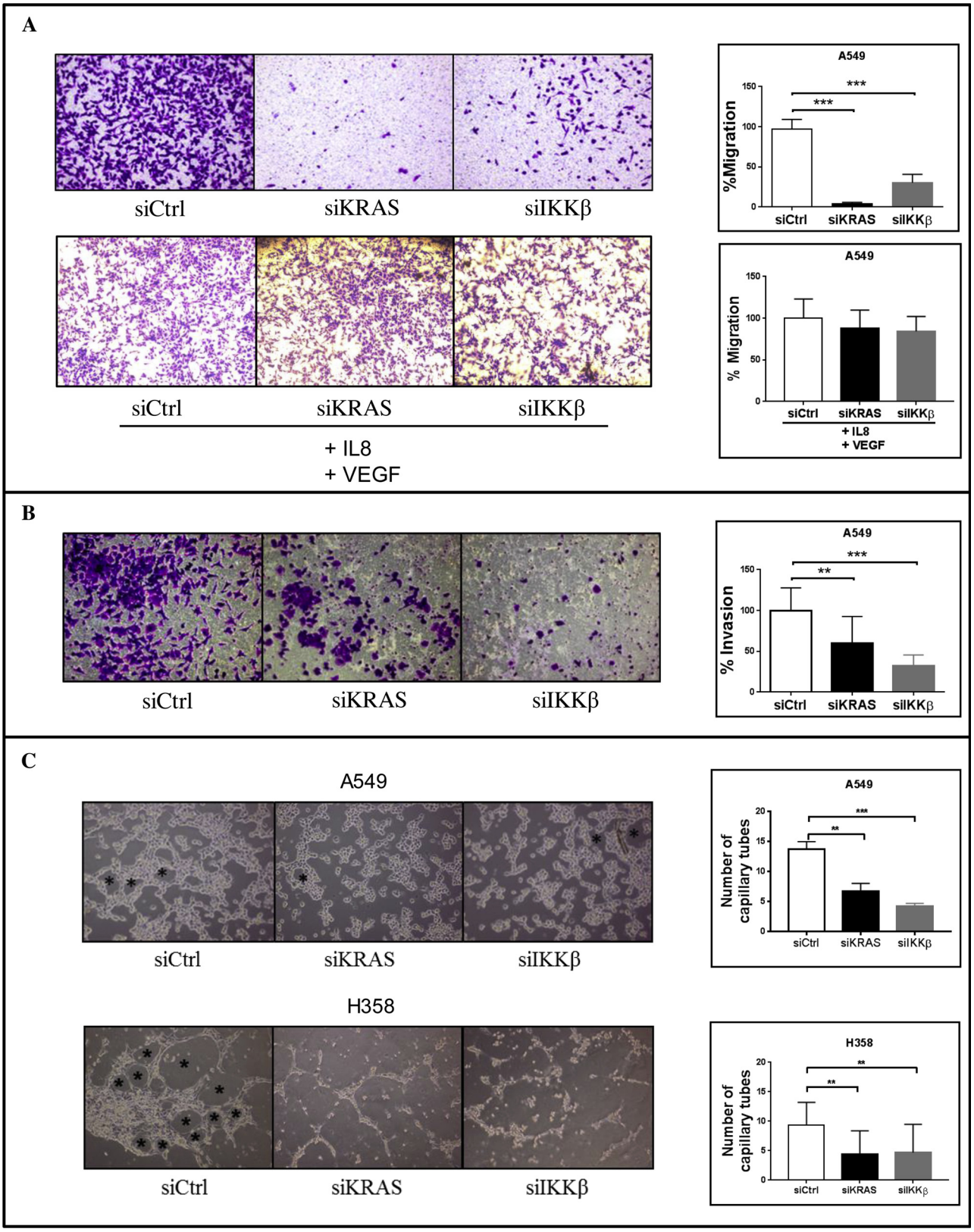

Fig. 2. siRNA-mediated inhibition of IKKβ expression decreases HUVEC migration, invasion and tube formation *in vitro*. A549 cells were transfected with a non-targeting control siRNA (siCtrl) or with siRNA smartpools targeting KRAS (siKRAS) or IKKβ (siIKKβ) and conditioned medium was collected as described in methods. (**a**) Transwell migration assay of HUVEC cells was performed using conditioned medium from A549-transfected cells as chemoattractant as indicated. Conditioned medium was supplemented with 5 ng/mL IL-8 and 5 ng/mL VEGF as indicated (lower panel). Images shown are representative of three independent experiments. (**b**) Transwell matrigel invasion assay of HUVEC cells was performed using conditioned medium from A549-transfected cells as chemoattractant as indicated. Images shown are representative of three independent experiments. (**c**) Endothelial cell tube formation assay. HUVEC cells were plated onto Matrigel in the presence of serum-free conditioned medium from A549- or H358-transfected cells as indicated. Images shown are representative of three independent experiments. In all cases, bar graphs represent average ± 1 s.d. Statistical significance was measured by one-way ANOVA followed by Bonferroni's post-test (**$p < 0.01$, ***$p < 0.001$) by comparing siCtrl-transfected groups with siKRAS- and/or siIKKβ-transfected groups. Groups being compared are indicated by horizontal bars.

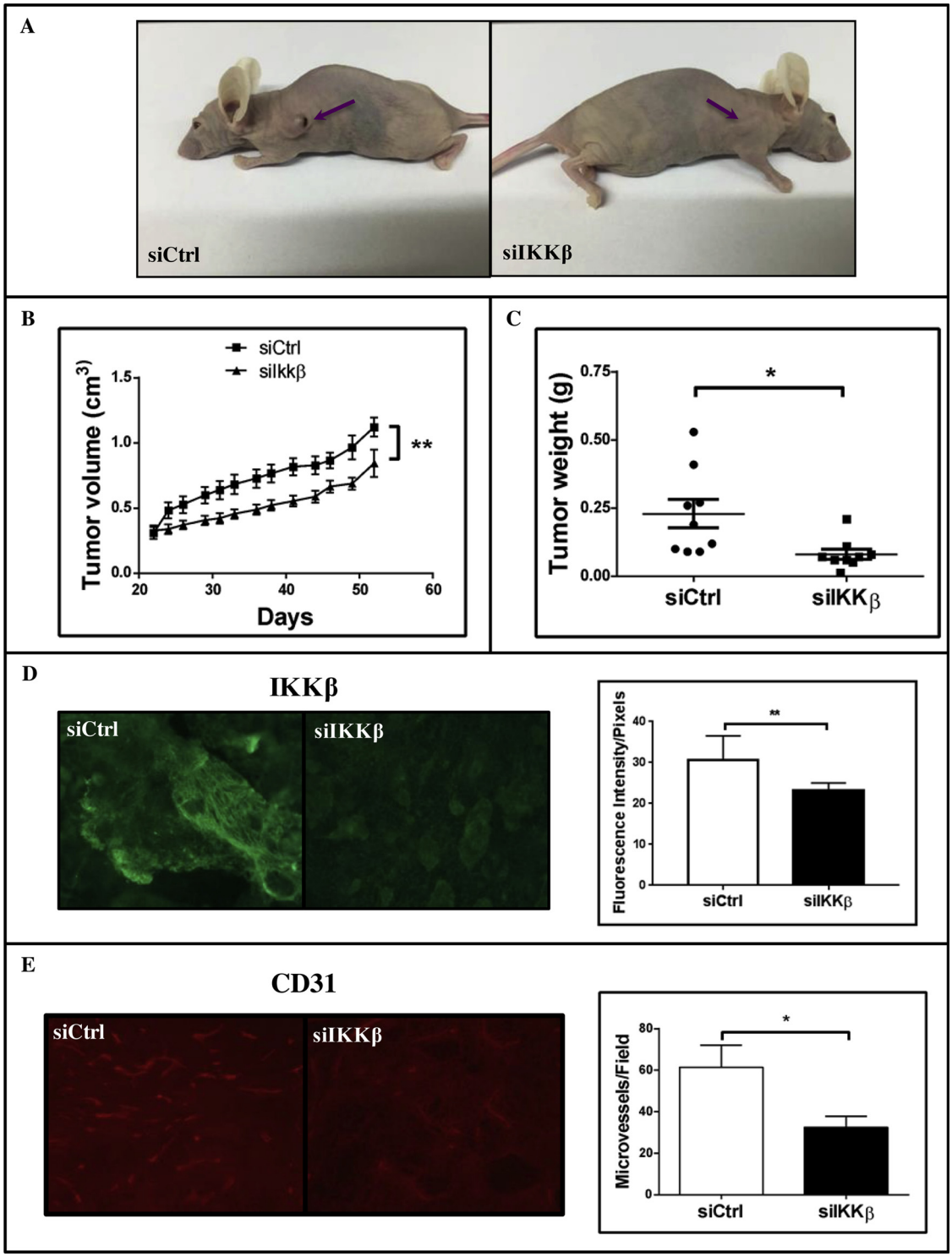

Fig. 3. siRNA-mediated inhibition of IKKβ expression decreases tumor growth and angiogenesis *in vivo*. 1×10^6 A549 cells transfected with a non-targeting control siRNA (siCtrl) or with a siRNA smartpool targeting IKKβ (siIKKβ) were injected subcutaneously into flanks of nude mice (n = 9 per group). (**a**) Representative images of tumor-bearing nude mice 55 days after inoculation. (**b**) Tumor growth kinetics assessed by tumor volume measurements overtime as indicated. Each point represents average ± 1 s.d. of each group. (**c**) Dot plot representing individual tumor weights 55 days after inoculation. Horizontal bars represent average weight in each group. (**d**) IKKβ expression was evaluated in tumor sections by immunostaining as described in methods. Right) Representative images of stained tumor sections. Left) Quantitation of IKKβ-staining intensity (right). **(e)** Vessel density was evaluated in tumor sections by immunofluorescence staining for CD31 as described in methods. Left) Representative images of stained tumor sections. Right) Quantitation of CD31-stained vessels. Statistical significance was determined by the Student's *t*-test (*$p < 0.05$) and the significantly different comparisons are indicated by vertical (**b**) or horizontal (**c, d**) bars. Error bars represent average ± 1 s.d.

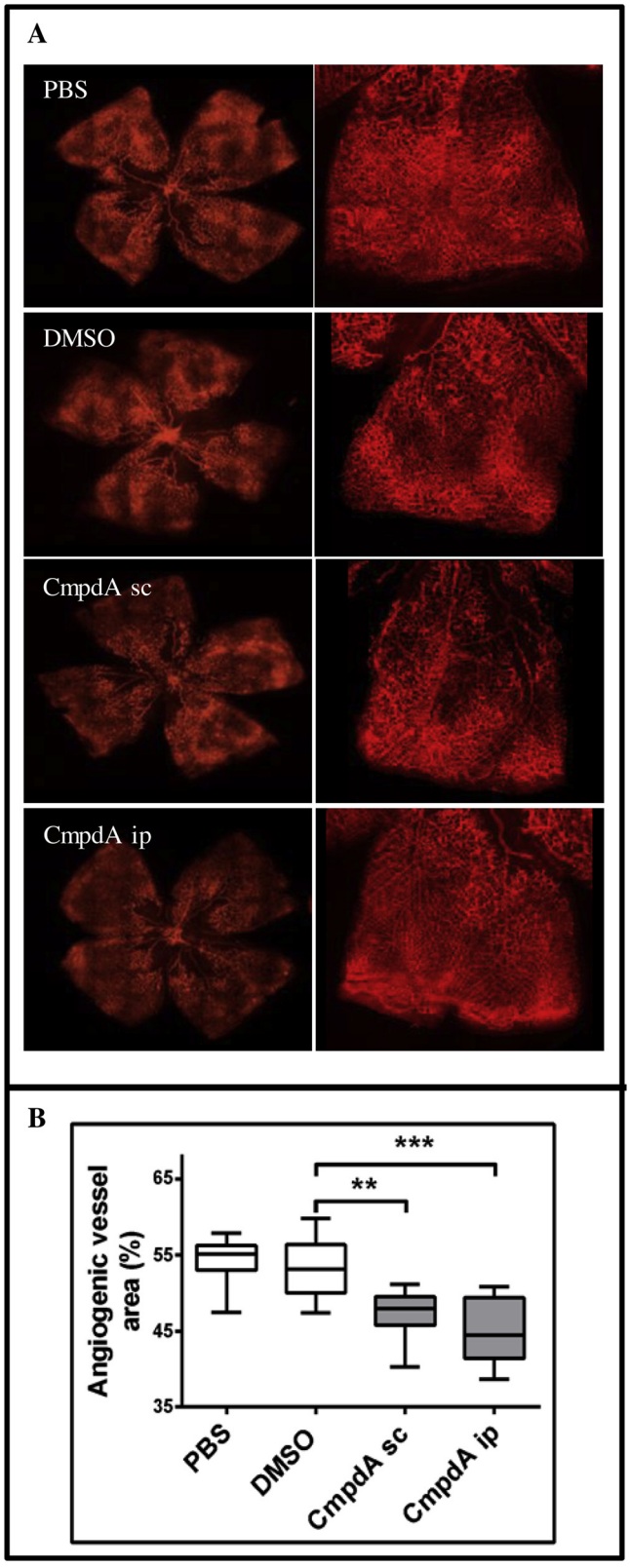

Fig. 4. IKKβ inhibition reduces pathological neovascularization in a cancer-independent oxygen-induced retinopathy (OIR) *in vivo* model. Newborn C57Black6 mice were submitted to the OIR protocol and treated with PBS (control), DMSO (vehicle control) or CmpdA as described in methods. Mice were euthanized at postnatal day 17 and their retinas were dissected and stained with GS-IB4 Isolectin, showing the neovascular tissue in different groups. (**a**) Representative images of Isolectin GS-IB4-stained retinas. High resolution images of retinal quadrants are depicted. (**b**) Quantitation of the isolectin GS-IB4-stained angiogenic area was performed as described in methods (n = 10 per group). PBS) Control PBS-treated mice; DMSO) Vehicle control DMSO-treated mice; CmpdA-sc) Mice treated with 10 mg/kg CmpdA subcutaneously; CmpdA-ip) Mice treated with 10 mg/kg CmpdA intraperitoneally. Statistical significance was measured by one-way ANOVA followed by Bonferroni's post-test (**p < 0.01, ***p < 0.001). Error bars represent average ± 1 s.d.

pathway is short-lived and limited by development of resistance followed by restoration of tumor growth and progression, likely due to activation of alternative proangiogenic pathways [36]. In that sense, dissecting the proangiogenic pathways induced by dominant oncogenes might uncover upstream signaling nodes that may control different proangiogenic pathways and provide better and more specific avenues to target tumor angiogenesis.

Dissection of proangiogenic pathways is particularly important for malignancies driven by the RAS oncogene, not only because oncogenic RAS is known to induce tumor angiogenesis, but also because RAS-driven malignancies are widespread and lack effective targeted therapies [3,4].

RAS-induced angiogenesis relies on the upregulation of proangiogenic factors VEGF and IL-8. In fact, VEGF or IL-8 targeting reduces RAS-induced angiogenesis and tumor growth [10,14,15]. Interestingly, VEGF and IL-8 have also been shown to be upregulated by the transcription factor NF-κB to promote glioblastoma angiogenesis [37], and we and others have shown that NF-κB activation by KRAS is required for KRAS-induced lung tumorigenesis [17,18]. Given that NF-κB activation by KRAS in the lung requires the IKKβ kinase [18], and that systemic IKKβ targeting reduced KRAS-induced lung tumor growth [23], we hypothesized that IKKβ, which is a druggable target in the KRAS-induced NF-κB activation pathway, would be involved in mediating KRAS-induced angiogenesis.

We show that both KRAS or IKKβ targeting reduces expression and secretion of IL-8 and VEGF in KRAS-mutant A549 and H358 cells (Fig. 1). Interestingly, IKKβ has been shown to promote VEGF and IL-8 expression in different studies [38–44]. For example, Lee et al. [38] have found that IKKβ promotes both transcriptional upregulation of VEGF expression, but also enhanced VEGF translation *via* mTOR and decreased VEGF expression is observed in IKKβ null MEFS [40]. Moreover, the IKKβ inhibitor IMD-0354 suppresses VEGF production from ovarian cancer cells *in vitro* and *in vivo* [42]. IKKβ has also been shown to promote IL-8 expression by binding to its promoter *via* interactions with p65 and EGR1 [43], and IKKβ targeting with CmpdA in primary immortalized lung epithelial cells transformed by KRAS reduces KRAS-induced IL-8 expression [18]. Our results, coupled with the abovementioned findings, corroborate the hypothesis that, in lung cancer, KRAS upregulates VEGF and IL-8 *via* IKKβ. Understanding this pathway is important because, in NSCLC, expression of both IL-8 and VEGF is associated with angiogenesis, lymph node metastasis, and unfavorable outcome [45–47].

Furthermore, conditioned medium from KRAS- or IKKβ-targeted cells reduced the ability of endothelial HUVEC cells to migrate in an IL-8 and VEGF-dependent manner, as well as invade and form tubular structures *in vitro* (Fig. 2). More importantly, siRNA-mediated IKKβ targeting reduced KRAS-positive lung xenograft tumor vascular density *in vivo* (Fig. 3). Even though IKKβ activity in endothelial cells is important for endothelial cell activation and vasculogenesis [21,48], and even though systemic IKKβ inhibition reduces ovarian xenograft tumor vascular density [42], our results show, for the first time, that efficient tumor angiogenesis in KRAS-mutant lung tumor xenografts requires cancer cell-intrinsic IKKβ activity.

Even though murine cells express a homolog of the IL-8 receptor, which responds to human IL-8, mice do not have an IL-8 homolog [28].

Mice do have functional IL-8 homologs (KC, MIP-2 and LIX), and the human counterparts of these homologs (CXCL1, CXCL2 and CXCL5) also play a role in human angiogenesis [49–51]. Nonetheless, considering that IL-8 is a critical mediator of RAS-induced angiogenesis [10], this important RAS-induced proangiogenic pathway can only be investigated in human models. Previously, we have shown that systemic treatment of murine KRAS-induced lung tumors with CmpdA was, not only able to block IKKβ activity in lung tumor cells *in situ*, but also reduced tumor vascular density [23]. Here, we show that IKKβ targeting also reduces vascular density of IL-8-secreting human lung tumor xenografts, thereby further validating IKKβ as an antiangiogenic therapeutic target for human KRAS-induced lung cancer.

In parallel to reducing vascular density, siRNA-mediated IKKβ targeting in KRAS-mutant A549 cells reduced lung tumor xenograft growth (Fig. 3), corroborating many studies that clearly show an important role for IKKβ in promoting oncogenesis [38,52–58]. More importantly, our results with human xenograft tumors also corroborate previous murine tumor studies showing that genetic or pharmacological IKKβ targeting reduces murine KRAS-induced lung tumor growth [22,23,59], thereby further underscoring IKKβ inhibition as a promising approach for KRAS-induced lung cancer therapy.

Nonetheless, when considering systemic cancer therapies, one must consider how target inhibition in normal cells, such as the ones present in the tumour microenvironment, might affect therapeutic outcome. The studies described above, where IKKβ was targeted systemically, cannot answer this question, because these studies cannot distinguish the effects of IKKβ inhibition in other cell types from cancer cell-intrinsic IKKβ inhibition. Interestingly, studies where IKKβ was specifically inhibited in different cell types show that, whereas IKKβ activity in endothelial cells is important for vasculogenesis [21] and myeloid-specific IKKβ activity promotes colon tumorigenesis [48], IKKβ activity in cancer-associated fibroblasts seems to actually have the opposite effect, suppressing angiogenesis and tumor growth [60]. Nonetheless, these studies also have limitations as they study IKKβ inhibition in specific cell compartments and do not take into account how simultaneous IKKβ targeting of these normal compartments would affect angiogenesis. Here we used a cancer cell-independent *in vivo* model of pathological angiogenesis, the oxygen-induced retinopathy (OIR) model [29,30]. Even though pathological angiogenesis in this model is not induced by KRAS, it can result in activation of the IKK/NF-κB pathway due to the relative hypoxia induced by the change in oxygen levels. In fact, NF-κB has been shown to be activated by hypoxia to promote angiogenesis [39,61]. Using this model, we show that systemic CmpdA therapy reduces pathological retinal neovascularization (Fig. 4).

This observation is important for two reasons. First, it indicates that CmpdA crosses the blood-brain barrier and might be a promising standalone or coadjuvant therapeutic approach to treat retinal diseases related to abnormal angiogenesis, such as diabetic retinopathy and age-related macular degeneration (AMD). In support of this idea, IKKβ inhibition in a mouse model of diabetic retinopathy decreased vessel leakage, thus preserving vascular integrity [62]. In addition, Lu et al. have shown that conditional deletion of IKKβ in the retina or intravitreal or retrobulbar injection of TPCA-1, an IKKβ inhibitor, reduced laser-induced choroidal neovascularization, which mimics the aberrant angiogenesis associated with AMD [63]. Contrary to TPCA-1, which was associated with significant toxicity [22], CmpdA is well tolerated in mice [23,24,64], and might therefore be a better option for AMD therapy.

Second and most important, our results suggest that systemic IKKβ inhibition might be an effective antiangiogenic therapy for KRAS-induced lung tumours, and maybe even for other KRAS-driven tumours, by acting both on cancer cells and on microenvironment cells to reduce angiogenesis.

In conclusion, we have identified IKKβ as a mediator of KRAS-induced angiogenesis in lung cancer in part by promoting secretion of proangiogenic factors VEGF and IL-8. Taken together, our results indicate that IKKβ promotes KRAS-induced angiogenesis by both cancer cell-intrinsic and cancer cell-independent mechanisms, which strongly suggests IKKβ inhibition as a promising antiangiogenic approach to be explored for KRAS-induced lung cancer therapy and possibly also for therapy of other KRAS-driven malignancies.

Conflict of interest

The authors declare that the research was conducted in the absence of any commercial or financial relationships that could be considered as potential conflict of interest.

Acknowledgements

This work was supported by a Young Investigator Grant (2010/52685-9) and a Research Grant (2016/19757-2) from the Fundação de Apoio à Pesquisa do Estado de São Paulo (FAPESP) to D.S.B., a NIH grant (1R35CA197684) to A.S.B., by a FAPESP postdoctoral fellowship to T.C.C-L, by Conselho Nacional de Desenvolvimento Científico e Tecnológico (CNPq) Ph.D. fellowships to E.O.S. and L.C.S. This work was also supported by the graduate program in Biochemistry and Molecular Biology of the University of São Paulo, which is sponsored by the Coordenação de Aperfeiçoamento de Pessoal de Nível Superior (CAPES, PROEX 1888/2016).

Appendix A. Supplementary data

Supplementary material related to this article can be found, in the online version, at doi:https://doi.org/10.1016/j.lungcan.2019.02.027.

References

[1] Y. Ohtaki, K. Shimizu, S. Kakegawa, T. Nagashima, T. Nakano, J. Atsumi, et al., Postrecurrence survival of surgically resected pulmonary adenocarcionama patients according to EGFR and KRAS mutation status, Mol. Clin. Oncol. 2 (2) (2014) 187–196, https://doi.org/10.3892/mco.2013.237.
[2] Z. Lohinai, T. Klikovits, J. Moldvay, G. Ostoros, E. Raso, J. Timar, et al., KRAS-mutation incidence and prognostic value are metastatic site-specific in lung adenocarcinoma: poor prognosis in patients with KRAS mutation and bone metastasis, Sci. Rep. 7 (2017) 39721, https://doi.org/10.1038/srep39721.
[3] A.G. Stephen, D. Esposito, R.K. Bagni, F. McCormick, Dragging ras back in the ring, Cancer Cell 25 (3) (2014) 272–281, https://doi.org/10.1016/j.ccr.2014.02.017.
[4] A.D. Cox, S.W. Fesik, A.C. Kimmelman, J. Luo, C.J. Der, Drugging the undruggable RAS: mission possible? Nat. Rev. Drug Discov. 13 (11) (2014) 828–851, https://doi.org/10.1038/nrd4389.
[5] J. Downward, RAS synthetic lethal screens revisited: still seeking the elusive prize? Clin. Cancer Res. 21 (8) (2015) 1802–1809, https://doi.org/10.1158/1078-0432.
[6] A.C. Kimmelman, Metabolic dependencies in RAS-driven cancers, Clin. Cancer Res. 21 (8) (2015) 1828–1834, https://doi.org/10.1158/1078-0432.
[7] D. Zeitouni, Y. Pylayeva-Gupta, C.J. Der, K.L. Bryant, KRAS mutant pancreatic cancer: no lone path to an effective treatment, Cancers (Basel) 8 (4) (2016) 45, https://doi.org/10.3390/cancers8040045.
[8] O. Kranenburg, M.F. Gebbink, E.E. Voest, Stimulation of angiogenesis by Ras proteins, Biochim. Biophys. Acta 1654 (1) (2004) 23–37, https://doi.org/10.1016/j.bbcan.2003.09.004.
[9] Y. Tang, M. Kim, D. Carrasco, A.L. Kung, L. Chin, R. Weissleder, In vivo assessment of RAS-dependent maintenance of tumor angiogenesis by real-time magnetic resonance imaging, Cancer Res. 65 (18) (2005) 8324–8330, https://doi.org/10.1158/0008-5472.CAN-05-0027.
[10] A. Sparmann, D. Bar-Sagi, Ras-induced interleukin-8 expression plays a critical role in tumor growth and angiogenesis, Cancer Cell 6 (5) (2004) 447–458, https://doi.org/10.1016/j.ccr.2004.09.028.
[11] Y. Matsuo, P.M. Campbell, R.A. Brekken, B. Sung, M.M. Ouellette, J.B. Fleming, et al., K-Ras promotes angiogenesis mediated by immortalized pancreatic epithelila cells through mitogen-activatd protein kinase signaling pathways, Mol. Cancer Res. 7 (6) (2009) 799–808, https://doi.org/10.1158/1541-7786.
[12] N. Sunaga, H. Imai, K. Shimizu, D.S. Shames, S. Kakegawa, L. Girard, et al., Oncogenic KRAS-induced interleukin-8 overexpression promotes cell growth and migration and contributes to aggressive phenotypes of non-small cell lung cancer, Int. J. Cancer 130 (8) (2012) 1733–1744, https://doi.org/10.1002/ijc.26164.
[13] M.M. Murillo, S. Zelenay, E. Nye, E. Castellano, F. Lassailly, G. Stamp, et al., RAS interation with PI3K p11α is required for tumor-induced angiogenesis, J. Clin. Invest. 124 (8) (2014) 3601–3611, https://doi.org/10.1172/JCI74134.
[14] F. Okada, J.W. Rak, B.S. Croix, B. Lieubeau, M. Kaya, L. Roncari, et al., Impact of

oncogenes in tumor angiogenesis: mutant K-ras up-regulation of vascular endothelial growth factor/vascular permeability factor is necessary, but not sufficient for tumorigenicity of human colorectal carcinoma cells, Proc. Natl. Acad. Sci. U. S. A. 95 (7) (1998) 3609–3614.
[15] J. Grunstein, W.G. Roberts, O. Mathieu-Costello, D. Hanahan, R.S. Johnson, Tumor-derived expression of vascular endothelial growth factor is a critical factor in tumor expansion and vascular function, Cancer Res. 59 (7) (1999) 1592–1598.
[16] D.S. Bassères, A.S. Baldwin, Nuclear factor-kappaB and inhibitor of kappaB kinase pathways in oncogenic initiation and progression, Oncogene 25 (51) (2006) 6817–6830, https://doi.org/10.1038/sj.onc.1209942.
[17] E. Meylan, A.L. Dooley, D.M. Feldser, L. Shen, E. Turk, C. Ouyang, et al., Requirement for NF-kappaB signaling in a mouse model of lung adenocarcinoma, Nature 462 (7269) (2009) 104–107, https://doi.org/10.1038/nature08462.
[18] D.S. Bassères, A. Ebbs, E. Levantini, A.S. Baldwin, Requirement of the NF-kappaB subunit p65/RealA for K-Ras-induced lung tumorigenesis, Cancer Res. 70 (9) (2010) 3537–3546, https://doi.org/10.1158/0008-5472.
[19] A. Duran, J.F. Linares, A.S. Galvez, K. Wikenheiser, J.M. Flores, M.T. Diaz-Meco, et al., The signaling adaptor p62 is an important NF-kappaB mediator in tumorigenesis, Cancer Cell 13 (4) (2008) 343–354, https://doi.org/10.1016/j.ccr.2008.02.001.
[20] Y. Hou, F. Li, M. Karin, M.C. Ostrowski, Analysis of the IKKβ/NF-kappaB signaling pathway during embryonic angiogenesis, Dev. Dyn. 237 (10) (2008) 2926–2935, https://doi.org/10.1002/dvdy.21723.
[21] N. Ashida, S. Senbanerjee, S. Kodama, S.Y. Foo, M. Coggins, J.A. Spencer, et al., Ikkβ regulates essential functions of the vascular endothelium through kinase-dependent and independent pathways, Nat. Commun. 2 (2011) 318, https://doi.org/10.1038/ncomms1317.
[22] Y. Xia, N. Yeddula, M. Leblanc, E. Ke, Y. Zhang, E. Oldfield, et al., Reduced cell proliferation by IKK2 depletion in a mouse lung-cancer model, Nat. Cell Biol. 14 (3) (2012) 257–265, https://doi.org/10.1038/ncb2428.
[23] D.S. Bassères, A. Ebbs, P.C. Cogswell, A.S. Baldwin, IKK is a therapeutic target in KRAS-induced lung cancer with disrupted p53 activity, Genes Cancer 5 (1–2) (2014) 41–55, https://doi.org/10.18632/genesandcancer.5.
[24] K. Ziegelbauer, F. Gantner, N.W. Lukacs, A. Berlin, K. Fuchikami, T. Niki, et al., A selective novel low-molecular-weight inhibitor of IkappaB Kinase-beta (IKKβ) prevents pulmonary inflammation and shows broad anti-inflammatory activity, Br. J. Pharmacol. 145 (2) (2005) 178–192, https://doi.org/10.1038/sj.bjp.0706176.
[25] J.S. Michaloski, A.R. Redondo, L.S. Magalhães, C.C. Cambui, R.J. Giordano, Discovery of pan-VEGF inhibitory peptides directed to the extracellular ligand-binding domains of the VEGF receptors, Sci. Adv. 2 (10) (2016) e1600611, https://doi.org/10.1126/sciadv.1600611.
[26] K.M. Connor, N.M. Krah, R.J. Dennison, C.M. Aderman, J. Chen, K.I. Guerin, et al., Quantification of oxygen-induced retinopathy in the mouse: a model of vessel loss, vessel regrowth and pathological angiogenesis, Nat. Protoc. 4 (11) (2009) 1565–1573, https://doi.org/10.1038/nprot.2009.187.
[27] S. Ziyad, M.L. Iruela-Arispe, Molecular mechanisms of tumor angiogenesis, Genes Cancer 2 (12) (2011) 1085–1096, https://doi.org/10.1177/1947601911432334.
[28] W.S. Modi, T. Yoshimura, Isolation of novel GRO genes and a phylogenetic analysis of the CXC chemokine subfamily in mammals, Mol. Biol. Evol. 16 (2) (1999) 180–193, https://doi.org/10.1093/oxfordjournals.molbev.a026101.
[29] L.E. Smith, E. Wesolowski, A. McLellan, S.K. Kostyk, R. D'Amato, R. Sullivan, et al., Oxygen-induced retinopathy in the mouse, Invest. Ophthalmol. Vis. Sci. 35 (1) (1994) 101–111.
[30] C.B. Kim, P.A. D'Amore, K.M. Connor, Revisiting the mouse model of oxygen-induced retinopathy, Eye Brain 8 (2016) 67–79, https://doi.org/10.2147/EB.S94447.
[31] R.J. Giordano, M. Cardó-Vila, A. Salameh, C.D. Anobom, B.D. Zeitlin, D.H. Hawke, et al., From combinatorial peptide selection to drug prototype (I): targeting the vascular endothelial growth factor receptor pathway, Proc. Natl. Acad. Sci. U. S. A. 107 (11) (2010) 5112–5117, https://doi.org/10.1073/pnas.0915141107.
[32] R.L. Sidman, J. Li, M. Lawrence, W. Hu, G.F. Musso, R.J. Giordano, et al., The peptidomimetic vasotide targets two retinal VEGF receptors and reduces pathological angiogenesis in murine and nonhuman primate models of retinal disease, Sci. Transl. Med. 7 (309) (2015), https://doi.org/10.1126/scitranslmed.aac4882 309ra165.
[33] D. Hanahan, R.A. Weinberg, Hallmark of cancer: the next generation, Cell 144 (5) (2011) 646–674, https://doi.org/10.1016/j.cell.2011.02.013.
[34] S.M. Weis, D.A. Cheresh, Tumor angiogenesis: molecular pathways and therapeutic targets, Nat. Med. 17 (11) (2011) 1359–1370, https://doi.org/10.1038/nm.2537.
[35] D.R. Bielenberg, B.R. Zetter, The contribution of angiogenesis to the process of metastasis, Cancer J. 21 (4) (2015) 267–273, https://doi.org/10.1097/PPO.0000000000000138.
[36] G. Bergers, D. Hanahan, Modes of resistence to anti-angiogenic therapy, Nat. Rev. Cancer 8 (8) (2008) 592–603, https://doi.org/10.1038/nrc2442.
[37] T.X. Xie, Z. Xia, N. Zhang, W. Gong, S. Huang, Constitutive NF-kappaB activity regulates the expression of VEGF and IL-8 and tumor angiogenesis of human glioblastoma, Oncol. Rep. 23 (3) (2010) 725–732.
[38] D.F. Lee, H.P. Kuo, C.T. Chen, J.M. Hsu, C.K. Chou, Y. Wei, et al., IKKβ suppression of TSC1 links inflammation and tumor angiogenesis via the mTOR pathway, Cell 130 (3) (2007) 440–455, https://doi.org/10.1016/j.cell.2007.05.058.
[39] J. Rius, M. Guma, C. Schachtrup, K. Akassoglou, A.S. Zinkernagel, V. Nizet, et al., NF-kappaB links innate immunity to the hypoxic response through transcriptional regulation of HIF-1alpha, Nature 453 (7196) (2008) 807–811, https://doi.org/10.1038/nature06905.
[40] H.P. Kuo, D.F. Lee, W. Xia, Y. Wei, M.C. Hung, TNFalpha induces HIF-1-alpha expression through of IKKβ, Biochem. Biophys. Res. Commun. 389 (4) (2009) 640–644, https://doi.org/10.1016/j.bbrc.2009.09.042.
[41] V.A. Londhe, T.M. Maisonet, B. Lopez, J.M. Jeng, J. Xiao, C. Li, et al., Conditional deletion of epithelial IKKβ impairs alveolar formation through apoptosis and decreased VEGF expression during early mouse lung morphogenesis, Respir. Res. 12 (2011) 134, https://doi.org/10.1186/1465-9921-12-134.
[42] Y. Kinose, K. Sawada, H. Makino, T. Ogura, T. Mizuno, N. Suzuki, et al., IKKβ regulates VEGF expression and is a potencial therapeutic target for ovarian cancer as an angiogenic treatment, Mol. Cancer Ther. 14 (4) (2015) 909–919, https://doi.org/10.1158/1535-7163.MCT-14-0696.
[43] B. Singha, H.R. Gatla, S. Manna, T.P. Chang, S. Sanacora, V. Poltoratsky, et al., Proteasome inhibition increases recruitment of IκB Kinase (IKKβ), S536P-p65, and transcription factor EGR1 to interleukin-8 (IL-8) promoter, resulting in increased IL-8 production in ovarian cancer cells, J. Biol. Chem. 289 (5) (2014) 2687–2700, https://doi.org/10.1074/jbc.M113.502641.
[44] B. Singha, H.R. Gatla, S. Phyo, A. Patel, Z.S. Chen, I. Vancurova, IKK inhibition increase bortezomib effectiveness in ovarian cancer, Oncotarget 6 (28) (2015) 26347–26358, https://doi.org/10.18632/oncotarget.4613.
[45] Y. Ohta, Y. Endo, M. Tanaka, J. Shimizu, M. Oda, Y. Hayashi, et al., Significance of vascular endothelial growth factor messenger RNA expression in primary lung cancer, Clin. Cancer Res. 2 (8) (1996) 1411–1416.
[46] Y. Ohta, Y. Watanabe, S. Murakami, M. Oda, Y. Hayashi, A. Nonomura, et al., Vascular endothelial growth factor and lymph node metastasis in primary lung cancer, Br. J. Cancer 76 (8) (1997) 1041–1045.
[47] A. Yuan, P.C. Yang, C.J. Yu, W.J. Chen, F.Y. Lin, S.H. Kuo, et al., Interleukin-8 messenger ribonucleic acid expression correlates with tumor progression, tumor angiogenesis, patient survival, and timing of relapse in non-small-cell lung cancer, Am. J. Respir. Crit. Care Med. 162 (5) (2000) 1957–1963, https://doi.org/10.1164/ajrccm.162.5.2002108.
[48] C. Iosef, M. Liu, L. Ying, S.P. Rao, K.R. Concepcion, W.K. Chan, et al., Distinct roles for IκB kinases alpha and beta in regulating pulmonary endothelial angiogenic function during late lung development, J. Cell. Mol. Med. 00 (2018) 1–13, https://doi.org/10.1111/jcmm.13741.
[49] D. Wang, H. Wang, J. Brown, T. Daikoku, W. Ning, Q. Shi, et al., CXCL1 induced by prostaglandin E2 promotes angiogenesis in colorectal cancer, J. Exp. Med. 203 (4) (2006) 941–951, https://doi.org/10.1084/jem.20052124.
[50] J. Hol, L. Wilhelmsen, G. Haraldsen, The murine IL-8 homologues KC, MIP-2, and LIX are found in endothelial cytoplasmic granules but not in Weibel-Palade bodies, J. Leukoc. Biol. 87 (3) (2010) 501–518, https://doi.org/10.1189/jlb.0809532.
[51] A. Li, J. King, A. Moro, M.D. Sugi, D.W. Dawson, J. Kaplan, et al., Overexpression of CXCL5 is associated with poor survival in patients with pancreatic cancer, Am. J. Pathol. 178 (3) (2011) 1340–1349.
[52] F.R. Greten, L. Eckmann, T.F. Greten, J.M. Park, Z.W. Li, L.J. Egan, et al., Ikkβ links inflammation and tumorigenesis in a mouse model of colitis-associated cancer, Cell 118 (3) (2004) 285–296.
[53] K. Makino, C.P. Day, S.C. Wang, Y.M. Li, M.C. Hung, Upregulation of IKKalpha/IKKbeta by integrin-linked kinase is required for HER2/neu-induced NF-kappaB antiapoptotic pathway, Oncogene 23 (21) (2004) 3883–3887, https://doi.org/10.1038/sj.onc.1207485.
[54] C. Frelin, V. Imbert, E. Griessinger, A.C. Peyron, N. Rochet, P. Philip, et al., Targeting NF-kappab activation via pharmacologic inhibition of IKK2-induced apoptosis of human acute myeloid leukemia cells, Blood 105 (2) (2005) 804–811, https://doi.org/10.1182/blood-2004-04-1463.
[55] T. Hideshima, P. Neri, P. Tassone, H. Yasui, K. Ishitsuka, N. Raje, et al., MLN120B, a novel Ikappab kinase beta inhibitor, blocks multiple myeloma cell growth in vitro and in vivo, Clin. Cancer Res. 12 (19) (2006) 5887–5894, https://doi.org/10.1158/1078-0432.CCR-05-2501.
[56] B. Ping, X. He, W. Xia, D.F. Lee, Y. Wei, D. Yu, et al., Cytoplasmic expression of p21CIP1/WAF1 is correlated with IKKβ overexpression in human breast cancers, Int. J. Oncol. 29 (5) (2006) 1103–1110.
[57] J. Yang, W.H. Pan, G.A. Clawson, A. Richmond, Systemic targeting inhibitor of kappaB kinase inhibits melanoma tumor growth, Cancer Res. 67 (7) (2007) 3127–3134, https://doi.org/10.1158/0008-5472.CAN-06-3547.
[58] J. Ling, Y. Kang, R. Zhao, Q. Xia, D.F. Lee, Z. Chang, et al., KrasG12D-induced IKK2/β/NF-κB activation by IL-1α and p62 feedforward loops is required for development of pancreatic ductal adenocarcinoma, Cancer Cell 21 (1) (2012) 105–120, https://doi.org/10.1016/j.ccr.2011.12.006.
[59] W. Xue, E. Meylan, T.G. Oliver, D.M. Feldser, M.M. Winslow, R. Bronson, et al., Response and resistence to NF-κB inhibitors in mouse models of lung adenocarcinoma, Cancer Discov. 1 (3) (2011) 236–247, https://doi.org/10.1158/2159-8290.CD-11-0073.
[60] C.K. Pallangyo, P.K. Ziegler, F.R. Greten, IKKβ acts as a tumor suppressor in cancer-associated fibroblasts during intestinal tumorigenesis, J. Exp. Med. 212 (13) (2015) 2253–2266, https://doi.org/10.1084/jem.20150576.
[61] L. D'Ignazio, M. Batie, S. Rocha, Hypoxia and inflammation in cancer, focus on HIF and NF-κB, Biomedicines 5 (2) (2017), https://doi.org/10.3390/biomedicines5020021 pii: E21.
[62] A. Lennikov, M. Hiraoka, A. Abe, S. Ohno, T. Fujikawa, A. Itai, et al., IκB Kinase-β inhibitor IMD-0354 beneficially suppresses retinal vascular permeability in streptozotocin-induced diabetic mice, Invest. Ophthalmol. Vis. Sci. 55 (10) (2014) 6365–6373, https://doi.org/10.1167/iovs.14-14671.
[63] H. Lu, Q. Lu, S. Gaddipati, R.B. Kasetti, W. Wang, M. Pasparakis, et al., IKK2 inhibition attenuates laser-induced choroidal neovascularization, PLoS One 9 (1) (2014) e87530, https://doi.org/10.1371/journal.pone.0087530.
[64] A. Wysong, M. Couch, S. Shadfar, L. Li, J.E. Rodriguez, S. Asher, et al., NF-κB inhibition protects again tumor-induced cardiac atrophy in vivo, Am. J. Pathol. 178 (3) (2011) 1059–1068, https://doi.org/10.1016/j.ajpath.2010.12.009.